Tunnelling and Underground Space Technology 41 (2014) 74–81

AN UPDATE OF THE "MULTIPLE GRAPH" APPROACH FOR THE PRELIMINARY ASSESSMENT OF THE EXCAVATION BEHAVIOUR IN ROCK TUNNELLING

G. Russo
Geodata Engineering (GDE), Corso Bolzano 14, Turin, Italy

ABSTRACT: The so-called "multiple graph" approach is a useful tool for the preliminary assessment of excavation behaviour in rock tunnelling, as well as to rationally select the pre-defined support section type at the tunnel face, during the construction phase. In a simplified but rational way the potential typical deformation phenomena (hazards) for tunnelling in rock are identified through the quantification, in a logical sequence, of fabric (1), strength (2), competency (3) and self-supporting capacity (4) of a rock mass. Based on this preliminary analysis, the tunnel design can consequently focus on the detected potential problems, implementing with the required detail the most adequate methods of analysis and calculations. In this paper, the fundamental bases of the method are summarized and some new considerations are presented.

1 INTRODUCTION

The "multiple graph" approach [31] is a useful tool either for the preliminary assessment of the excavation behaviour in rock tunnelling and, as it has been experienced [2,8,12,20,26] to select the support class to be applied at the tunnel face on the basis of the pre-defined design criteria.

In particular, the so-called "GDE multiple graph", reported in Fig. 1, is a 4-sector graph based on the logical sequence of the engineering steps in Table 1.

Graph 1	Rock block volume + Joint Conditions = Rock mass fabric
Graph 2	Rock mass fabric + Strength of intact rock = Rock mass strength
Graph 3	Rock mass strength + In situ stress = Competency
Graph 4	Competency + Self-supporting capacity = Excavation behaviour (→Potential hazards)

Table 1: Logical frame adopted for the identification of the excavation hazards.

In the next section, the technical bases of each equation are summarized, pointing out the relative background of each sector. At the same some new considerations are remarked.

2 THE GDE MULTIPLE GRAPH

As previously mentioned, the multiple graph is composed by 4 sectors (Fig. 1), each of them finalized to a user-friendly quantification of the corresponding properties presented in Tab. 1. The first graph is in the lower right quadrant and progress is clockwise through system.

2.1 *Graph I: Estimation of Rock Mass Fabric*

Graph I (lower right quadrant in Fig.1) estimates Rock Mass Fabric (GSI) based on Rock Block Volume (Vb) and Joint Conditions (jC).

When the rock mass can be reasonably treated as an equivalent-continuum, with isotropic geomechanical properties, the geo-structural features of rock masses can be expressed by a "fabric index" [33], which may be defined as a scalar function of two components: rock structure and joint condition. In the present case, the reference fabric index is the GSI and its estimate is derived by the method proposed by the author [30,32].

Such a new method for calculating the GSI has been developed taking into consideration the conceptual equivalence between GSI and JP (Jointing Parameter) of the RMi system [24,25], considering that both are used to scale down the intact rock strength (σ_c) to rock mass strength (σ_{cm}).

In fact, according with the two systems, we have:

RMi: $\sigma_{cm} = \sigma_c * JP$ (1)

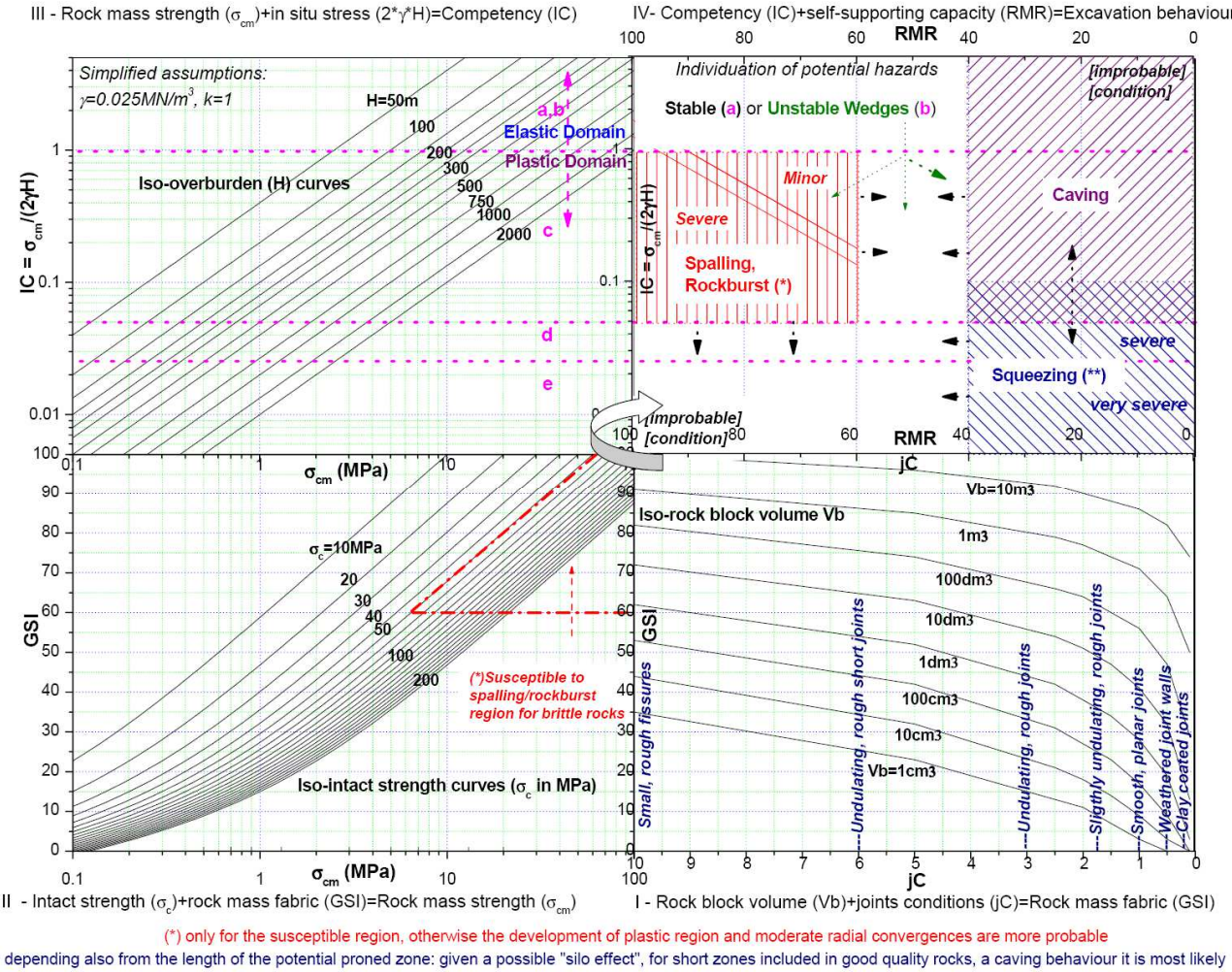

Fig.1: The GDE multiple-graph for the preliminary setting of excavation behaviour. Notes: (*) Only for the susceptible to spalling/rockburst region for brittle rocks [IF=(σ_c/σ_t)>8], otherwise a shear type failure should occur; the two new lines remarking the expected intensity of the brittle phenomenon are explained in the section 2.4. (**) Squeezing involves pronounced time-dependent deformations and is associated to rocks with low strength and high deformability: otherwise, prevalent plastic deformations (no time-dependent) occur, frequently associated to caving; squeezing depends also from the length of the potential prone zone: given a possible "wall effect" [1], for short zones included in good quality rocks, a caving behaviour is most likely to occur. Symbols: σ_c, σ_{cm}= intact, rock mass strength (=σ_c*s^a); jC= joint condition factor, Vb= block volume; γ= rock mass density.

GSI: $\sigma_{cm} = \sigma_c*s^a$ (2)

where s and a are the Hoek-Brown constants [13,17].

Therefore, JP should be numerically equivalent to s^a and given that for undisturbed rock masses [17] one has:

$s = \exp[(GSI-100)/9]$ and (3)

$a = (1/2)+(1/6)*[\exp(-GSI/15)-\exp(-20/3)]$ (4)

a direct correlation between JP and GSI can be obtained, i.e.:

$JP=[\exp((GSI-100)/9)]^{(1/2)+(1/6)*[\exp(-GSI/15)-\exp(-20/3)]}$ (5)

For the inverse derivation, the perfect correlation ($R^2 = 0.99995$) can be used with a sigmoidal (logistic) function of the type:

$GSI = (A1-A2)/[1+(JP/X_0)^p]+A2$ (6)

with A1=-12.198; A2=152.965; X_0=0.191; p=0.443. Then $GSI \approx 153-165/[1+(JP/0.19)^{0.44}]$ (7)

Based on such a correlation, a "robust" quantitative estimation of the GSI can be made, by defining the parameters concurrent to the evaluation of JP, i.e. the block volume (Vb) and the Joint Condition factor (jC). A graphic representation of the described correlation is presented in Fig. 2.

The sector I of the graph shown in Fig. 1 is derived from the above equations. The quantification of the Joint Condition Factor (jC) is based on published tables (see for example Palmstrom's web site www.rockmass.net, where a complete treatment of the RMi method can be found). Following the suggestion of Palmstrom [25], some typical jC values are reported in the graph as well for a quick preliminary evaluation.

Finally, it should be noted that the use of the described (GRS) approach is not recommended in complex and heterogeneous rock masses, such as a flysch, where the specific charts proposed by Marinos and Hoek [22] may be a more opportune reference for calculating the GSI.

2.2 *Graph II: Estimation of rock mass strength*

Graph II (lower left quadrant in Fig.1) estimates the Rock mass strength (σcm) based on Rock Mass Fabric (GSI) and Intact rock strength (σc)

The estimation of the rock mass strength is based on the equations of Hoek et al. [17], already presented above. In particular, such a value is graphically obtained by the intersection of the estimated GSI and intact strength curves. The reliability of the rock mass strength estimation is primarily related to both the effective applicability of the Hoek-Brown failure criterion (based on an assumed homogeneous and isotropic medium) and the occurrence of shear type failure. Differently, a "spalling type" failure, which involves intact rock strength, may occur when overstressing a good quality, hard and brittle rock mass. In such a case, according to the spall prediction approach" [9,10,11,19], the mobilized strength at failure may result either some higher and lower than the σ_{cm} derived by the GSI-based Hoek et al. equations [17], basically depending on the value of both the GSI itself and the stress for the cracks initiation.

For a preliminary estimation of the possibility of stress-driven instabilities of brittle rocks [Brittle Index IF= (σ_c/σ_t)>8], in the graph II, the region susceptible to spalling/rockburst, if in the presence of adequate stress conditions, is highlighted.

Taking into consideration the cited references, the lower boundaries of such a region have been taken in favour of safety as coincident with values of GSI and σ_c (MPa) both correspondent to 60.

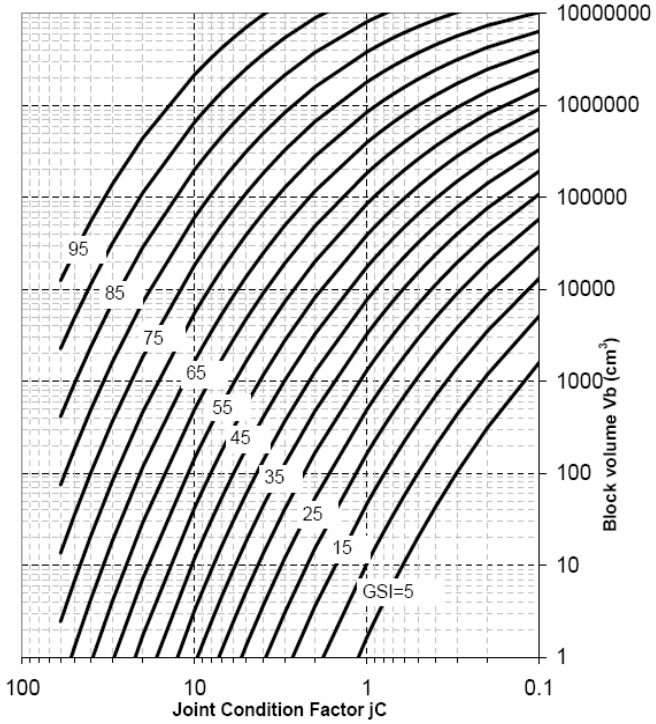

Fig. 2: Diagram for the assessment of GSI based on the RMi parameters jC and Vb [30,32].

2.3 *Graph III: Estimation of rock mass competency*

Graph III (upper left quadrant in Fig.1) estimates the Rock mass competency (IC) based on Rock mass strength (σ_{cm}) and In situ stress (σ_θ)

The Competency Index (IC) is simply defined as the ratio between the rock mass strength (σ_{cm}) and the tangential stress (σ_θ) on the excavation contour.

It is important to note that a simplified assumption about the original in-situ stress is here adopted by considering a value of k=1, where k is the ratio between the in situ horizontal and vertical principal stresses.

Consequently, for a circular tunnel one has $\sigma_\theta = 2\gamma H$, with γ= rock mass density (assumed value = 0.025MN/m^3) and H= overburden. In the case of k≠1 and/or $\gamma \neq 0.025$MN/m^3 a reasonable approximation may consist in calculating the maximum tangential stress $\sigma_{\theta max}=(3\sigma_1-\sigma_3)$ and then divide the result by 2γ (i.e by 0.05), in order to derive the fictitious overburden that origins the same $\sigma_\theta = \sigma_{\theta max}$ for k=1 and γ=0.025MN/m^3. Consequently, the classification point will be plotted as referring to the correspondent fictitious overburden.

The value of IC=1 separates in the graph the deformation response of the excavation into the elastic (above) and plastic (below) domains.

Moreover, in the graph are also reported some horizontal dotted lines which represent the best correlation of the Competency Index with the GDE behavioural classification reported in Fig. 5 [28,29,32].

As later presented (Fig. 5), in such a classification four classes (a/b, c, d, e/f) were originally identified [27] as function of both the radial deformation at the excavation face (δ_o) and the normalized extension of the plastic zone around the cavity (Rp/Ro).

Two further distinctions were considered: 1) in the case of elastic response (i.e. classes a/b) the class "b" indicated a discontinuous rock mass prone to wedge instability; 2) the class "f" was associated to conditions of immediate collapse of the tunnel face.

As treated in the next section, more recently the original GDE-classification has been updated to better take into account the real discontinuous character of the rock masses and consequently to improve the prediction of different deformation phenomena, such as the gravitational type and the brittle, stress-driven instabilities (Figs. 4, 5).

To transfer such a classification on the graph, the characteristic line [7] and the Monte Carlo methods have been implemented to find an approximate correlation between the IC and the GDE-classes.

In particular, as reported in Fig. 3, a large variability of the input geomechanical parameters has been considered by referring to adequate uniform distribution. Moreover, for the calculations:

i) a strain-softening behaviour has been considered by referring to the approach proposed by Cai et al. [6] centred on the concept of "residual GSI" (GSI_{res});

ii) the rock mass modulus of deformability has been derived by the simplified equation proposed by Hoek and Diederichs [14];

iii) δ_o has been obtained by the equation proposed by Hoek et al. [15].

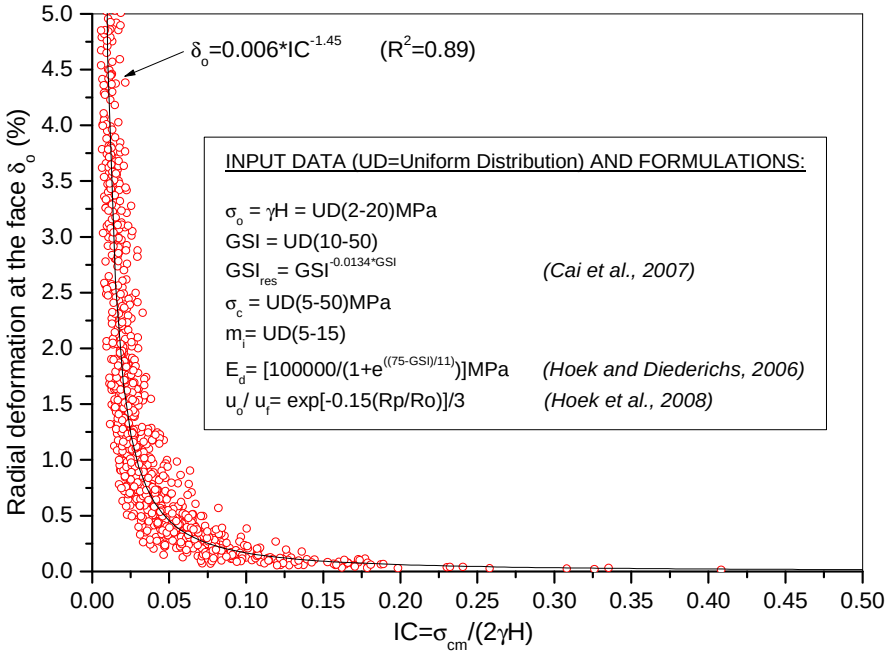

Fig. 3: Updated correlation between the radial deformation at the face (δ_o) and the Competency Index (IC). Note: u_o,u_f = radial displacement at tunnel face, final.

In Fig. 3, the results of 2000 iterations by the Latin Hypercube sampling method, as well as the best interpolating curve are shown for the relationship IC-δo.

Moreover, the combined state of the two parameters involved in the GDE classification (i.e. δo and Rp/Ro) has been analysed and the approximate correlation lines reported in the graph have been finally assessed.

Given the related uncertainty, the correlation reported in the multiple graph reflects only the most probable conditions for the parametrical variability assumed in the probabilistic calculation.

2.4 *Graph IV: Estimation of excavation behaviour*

Graph IV (upper right quadrant in Fig.1) estimates the Excavation Behaviour based on Rock mass competency (IC) and Self-supporting capacity (RMR).

In the last quadrant of the multiple graph, the integrated behavioural classification is applied in approximate form, by using the previous correlations with IC.

Following the conceptual scheme presented in Fig. 4, the original GDE-classification system has been integrated [4,5] by the RMR classes (Fig. 5) considering also their well-known empirical relationship with the self-supporting capacity of the rock masses.

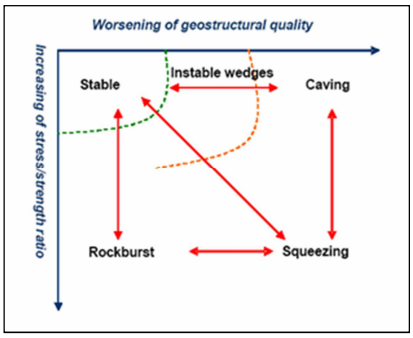

Fig. 4: Conceptual scheme for a general setting of the ground behaviour upon excavation

With the same logic of Fig. 4, some of the main hazards for tunnelling are consequently delimited in the new graph reported in the Fig. 5.
The term *caving* is here used to identify generic gravitational collapse of portions of highly fractured rock mass from the cavity and/or tunnel face. Therefore, given their very poor self-supporting capacity, the highest risk of caving is associated to the most unfavourable RMR classes.

Squeezing (s.s.) involves pronounced time-dependent deformations and is generally associated to rocks with low strength and high deformability such as, for example, phillytes, schists, serpentines, mudstones, tuffs, certain kinds of flysch, chemically weathered igneous rocks [17]. Otherwise, plastic deformations should prevail and caving is also probable. Further detailed analysis, based on a more accurate modelling of geomechanical properties, should be able to remark the just described distinction.

The terms “severe” and “very severe” have been associated to GDE-classes “d” and “e”, respectively. By considering also the type of stabilisation measures applied, they may be roughly related to the correspondent δ_f–based classes of squeezing proposed by Hoek and Marinos [16], if one incorporates in the last term also the grade “extremely severe”.

↓ANALYSIS→		Geostructural →		Rock mass				
				Continuous ↔	Discontinuous ↔			Equivalent C.
Tensional↓				RMR				
Deformational response ↓	δ_o (%)	Rp/Ro	Behavioural Category ↓	I	II	III	IV	V
Elastic ($\sigma_\theta<\sigma_{cm}$)	negligeble	-	a	STABLE				
			b		UNSTABLE WEDGES			CAVING
Elastic - Plastic ($\sigma_\theta\geq\sigma_{cm}$)	<0.5	1-2	c	SPALLING/ ROCKBURST				
	0.5-1.0	2-4	d					
	>1.0	>4	e					SQUEEZING
			(f)	→Immediate collapse of tunnel face↑				

Fig. 5: GDE classification scheme of the excavation behaviour [28,29,32]

Notes: δo=radial deformation at the face; Rp/Ro=plastic radius/radius of cavity; σ_θ=max tangential stress; σ_{cm}=rock mass strength. The limits of shadow zones are approximated and represent the most typical condition; see also the notes to Fig. 1 and further explanations in the text.

With respect to the original version, two lines have been added in the *spalling*/*rockburst* region to remark the potential intensity of the brittle phenomenon. This indication is based on the approximation that for very good rock the RMR rating could be assumed equal to the GSI. Consequently, either the GSI-based equation $\sigma_c=\sigma_{cm}/s^a$ (2) and the empirical relationship proposed by Martin et al. [23] between the ratio σ_θ/σ_c and the expected depth of failure (dof) have been considered (r=tunnel radius):

$$dof/r = 1.25(\sigma_\theta/\sigma_c)-0.51 \quad (8)$$

In particular, the classification proposed by Diederichs et al. [11] has been implemented, reporting in the graph the equivalent lines for minor and severe intensity of the brittle failure:

- "minor spalling" (σ_θ/σ_c <0.6 ↔ dof/r <0.25)
- "serious overbreak" (σ_θ/σ_c >0.8 ↔ dof/r >0.5)

It is important to observe that the depth of failure (dof) does not necessarily imply (or not only) a violent phenomenon ("rockburst"), which mainly depends to the rock strength and its related capacity to store energy.

The potential of *rock wedge* failure is mainly associated to good (/fair) rock masses subjected to relatively low stress condition, i.e. when the response at excavation is dominated by the shear strength of discontinuities and a "translational" failure should occur [3]. Further detailed analyses, for example by using limit equilibrium methods, should verify the effective possibility of kinematical instabilities.

Two "improbable" zones have also been marked in the graph corresponding to unrealistic combinations between GSI and RMR: the first below the "spalling/rockburst" region and the other in the upper right part ("caving" zone), where RMR class V and elastic behaviour theoretically overlap.

2.4.1 *Some remarks on the RMR assessment*

In the case that the RMR [4,5] values are not available for the application of the multiple graph, it may be useful to consider the procedure described in the following.

The RMR results by the sum of the following ratings:

r1=uniaxial rock strength
r2=RQD
r3=spacing of discontinuities
r4=condition of discontinuities
r5=groundwater condition
r6= adjustment for discontinuity orientation

Accordingly to Tzamos and Sofianos [33], the parameters r2, r3 and r4 represent the geostructural component of RMR and their sum is therefore conceptually equivalent to the GSI ("fabric index"). Consequently, given that the possible ranges of variability are 8 to 70 and 5 to 100, respectively, the following approximate equation can be derived:

$$(r2+r3+r4) \approx 0.65GSI+5 \quad (9)$$

or, more in general

$$RMR \approx 0.65GSI+5+r1+r5+r6 \quad (10)$$

In the Fig. 6 the reliability of the equation (9) is checked by the data collected with n. (257+188) face mappings realized in two tunnels crossing volcanic/igneous rocks (Andean mountains), actually under construction.

Consequently, as remarked by the equation (10), taking into account that either GSI and σ_c are known, the RMR can be reasonably assessed by estimating the two remaining parameters (r5 and r6), i.e. the expected groundwater condition (for tunnel below the water table, frequently related to the geostructural conditions and then to the GSI itself) and the correction for the orientations of the discontinuities with respect the tunnel advancement, respectively.

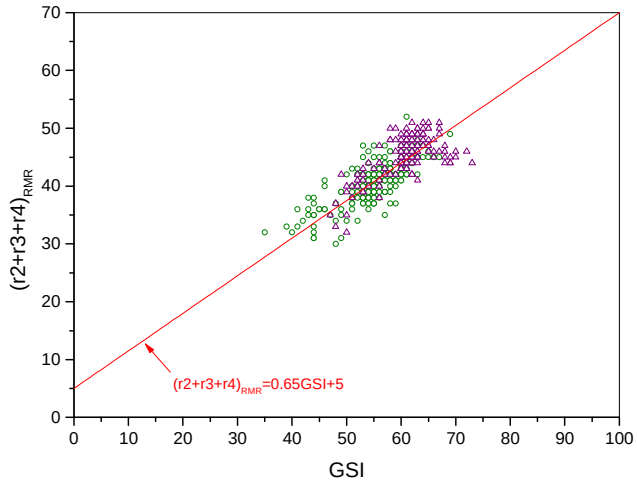

Fig. 6: Check of the proposed relationship between the GSI and the RMR geostructural component (r2+r3+r4) on the basis of n.(257+188) face mappings collected during the construction of two tunnels crossing volcanic/igneous rocks (Andean mountains). It is important to remember that the reference equation is based on the classification ratings of the involved parameters.

3 PRACTICAL APPLICATION OF THE MULTIPLE GRAPH

As remarked in the introduction, the multiple graph has two main field of application:

1) In the preliminary design phases to assess the expected excavation behaviour and related hazards, in order also to orient the successive detailed analysis;
2) in the construction phase, to select at the tunnel face the support section type to be applied in function of the encountered geomechanical condition. Consequently in the fourth quadrant the pre-defined field of application of the support section types are remarked according the design criteria of reference.

In the Figg. 7 and 9 some examples of application are reported with reference to these two practical options.

In particular, the graph in the Fig. 7 refers to the preliminary analysis for a zone of tunnel of 740m crossing igneous rock masses with an overburden of about 1000m and in presence of anisotropic in situ stress (k=1.5). Consequently, according to the procedure previously described, a fictitious overburden of about 1700m is considered to simulate the max stress at the tunnel crown and invert.

Taking into account the hypothesized variability of the main geomechanical parameters by adequate distributions, a probabilistic analysis (MonteCarlo method) has been performed and the results graphically presented (note that the GSI was already estimated and therefore the first quadrant is not compiled).

Given the high variability of the rock mass quality (GSI~20÷80) and generalized overstress conditions, the following main hazards should be expected:

- 20% moderate/severe spalling/rockburst;
- 50% severe/very severe squeezing

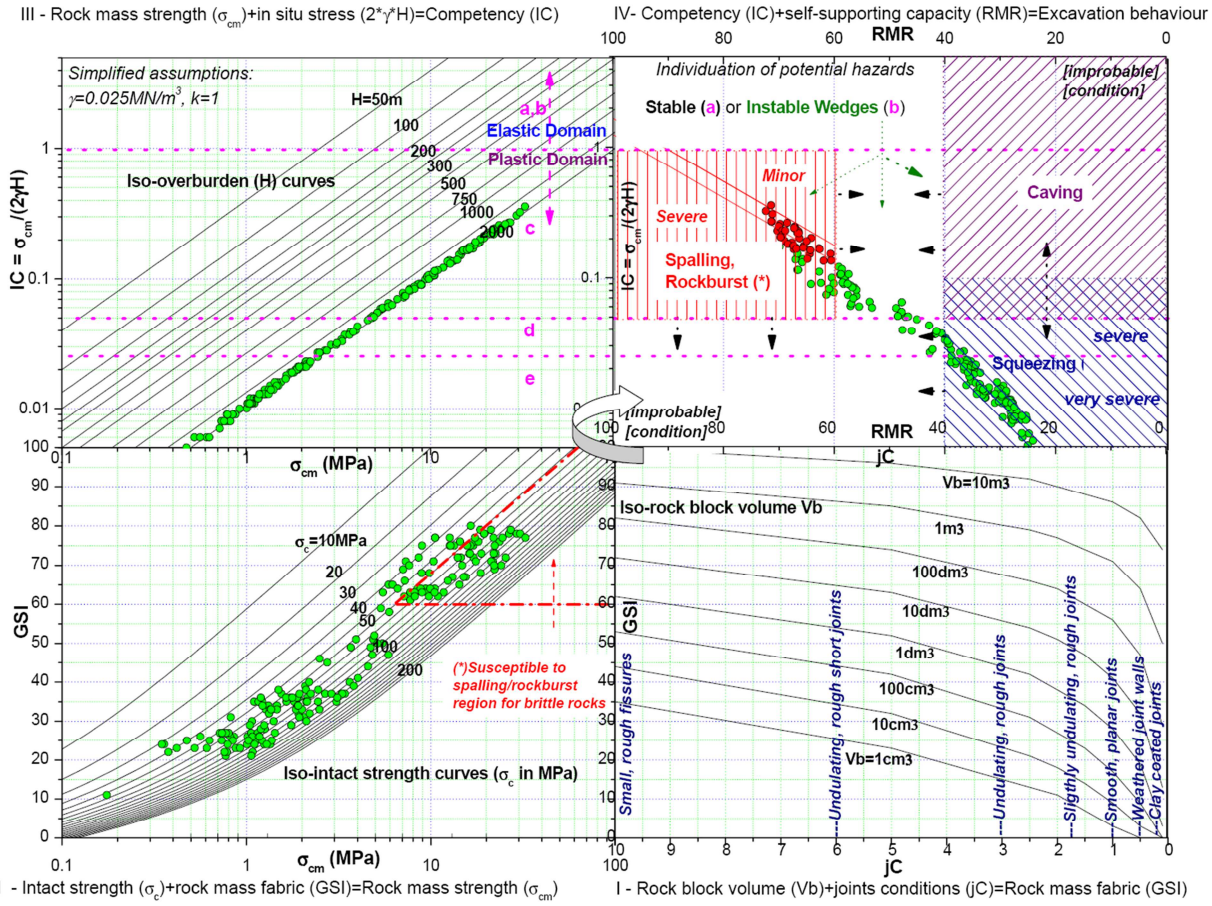

Fig. 7: Example 1 of multiple graph application: Probabilistic analysis for a tunnel zone of 740m in igneous rock mass (see details in the text).

Note: the red symbols remark the cases falling in the "Susceptible to spalling/rockburst region" in the II quadrant and therefore effectively subjected to such a hazard if in condition of overstressing.

It appears rational that in the development of the structural design some specific mitigation measures are associated to the different type of hazards and relative intensity. Therefore, the dimensioning of the stabilization measures and the consequent composition of the support section type derive by the selection of the most adequate design actions [28], either in advance and during the tunnel excavation. In the Fig. 8, as one example, some typical mitigation measures are listed and combined to guarantee the most adequate section types to each expected geomechanical hazards.

Following the same logic, in the Fig.9 the different section types of support systems are localized in the multiple graph, covering the correspondent field of application in the 4th quadrant.

During the construction phase, the main geomechanical parameters are defined at the tunnel face and the support section type to apply is consequently identified (see the example in the figure).

It is evident that diverse criteria can be analogously implemented, reflecting the defined combination of the main geomechanical parameters and therefore the specific approach of different designers.

Code	EXAMPLE OF RISK MITIGATION (STABILIZATION) MEASURES FOR TUNNEL [D&B]
	a) In advancement to the excavation
Ma1	Controlled drainage ahead the tunnel face/contour
Ma2	Pre-confinement/reinforcement of instable rock wedges (inclined bolts, spiling,..)
Ma3	Pre-confinement of excavation contour (reinforced grouting, jet grouting,..)
Ma4	Pre-reinforcement of rock mass contour (by fully connected elements)
Ma5	Pre-support of excavation contour (forepoling, umbrella arch,..)
Ma6	Tunnel face pre-reinforcement (injected fibreglass elements, reinforced grouting, jet gr..)
Ma7	Grouting for water-tightness
Ma8	De-stressing holes/blasting
.....	.....
	b) During the excavation
Mb1	Over-excavation to allow convergences (stress relief)
Mb2	Controlled de-confinement to allow convergences (sliding joints, deformable elements,..)
Mb3	Radial confinement of instable rock wedges
Mb4	Radial rock reinforcement (fully connected elements)
Mb5	Confinement by differently composed system (steel ribs, fbr shotcrete, bolts,..)
Mb6	High energy adsorbing composed system (steel mesh, yielding bolts, fbr shotcrete,..)
Mb7	Tunnel face protection
Mb8	Additional protective measures
.....	.....

Prevalent Hazard		GC		Excavation behaviour	ST	Typical mitigation measures
Gravity driven	Stress induced	GDE	RMR			
H1	Wedge instability/ Rockfall	a	I	Stable rock mass, with only possibility of local rock block fall; rock mass of very good quality with elastic response upon excavation	A	Ma1-Mb3
		b	II	Rock wedge instability; rock mass of good quality with elastic response upon excavation	B	Ma1-Mb3
		c	III	Pronounced tendency to rockfall; rock mass of fair quality, with possible occurrence of a moderate development of plastic zone	C1	Ma1-Mb5
H2	Spalling/ Rockburst	c	I-II	Mild brittle failure even associated to rock minor rock block ejection; overstressed hard, good rock mass (→Minor spalling/rockburst)		
		c	I-II	Sudden brittle failure; overstressed hard, good rock mass (→Moderate spalling/rockburst).	C3	Ma1-Mb6-Mb7
		c	I-II	Sudden and violent brittle failure, even associated to rock block ejection; highly overstressed hard, good rock mass (→Severe spalling/ heavy rockburst)	C4	Ma1-(Ma5) (Ma8)-Mb6-Mb7-Mb8
H3	Plastic deformations / Squeezing	d	III-IV-(V)	Development of plastic/viscous deformations; overstressed fair to poor rock mass, resulting in a significative extrusion of tunnel face and radial convergences (→Severe Squeezing)	D	Ma1-Ma5 (Ma6) (Mb4)-Mb5-Mb7
		e	III-IV-(V)	Intense development of plastic/viscous deformations; overstressed fair to poor rock mass, resulting in a large extrusion of tunnel face and radial convergences (→Very Severe Squeezing)	E	Ma1-Ma4 Ma6-Mb1-Mb2-Mb4-Mb5-Mb7
H4	Caving/ Flowing ground	c	IV	Gravity-driven instability; reduced self-supporting capacity of poor rock mass, generally associated to a moderate development of plastic zone	C2	Ma1 Ma5 (Ma6) Mb5-Mb7
		(e)/f	V	Severe gravity-driven instability, with immediate collapse of the tunnel face/excavation contour, including flowing ground; very poor quality, cataclastic rock mass, generally under conditions of high hydrostatic pressure/water inflow (fault zones, etc.)	F/ F_E	Ma1-Ma3 Ma5-Ma6 (Ma7) Mb5/(Mb2)-Mb7-Mb8

Note: GC=Geomechanical Classification; ST=Section Type

Fig. 8: On the left, one example of typical mitigation (stabilization) measures for D&B rock tunnelling; on the right, the GDE general rational for associating the different Section Types of support to the expected geomechanical hazards and relative intensity. According to the hazard specificity, adequate calculation methods are consequently adopted for the structural design.

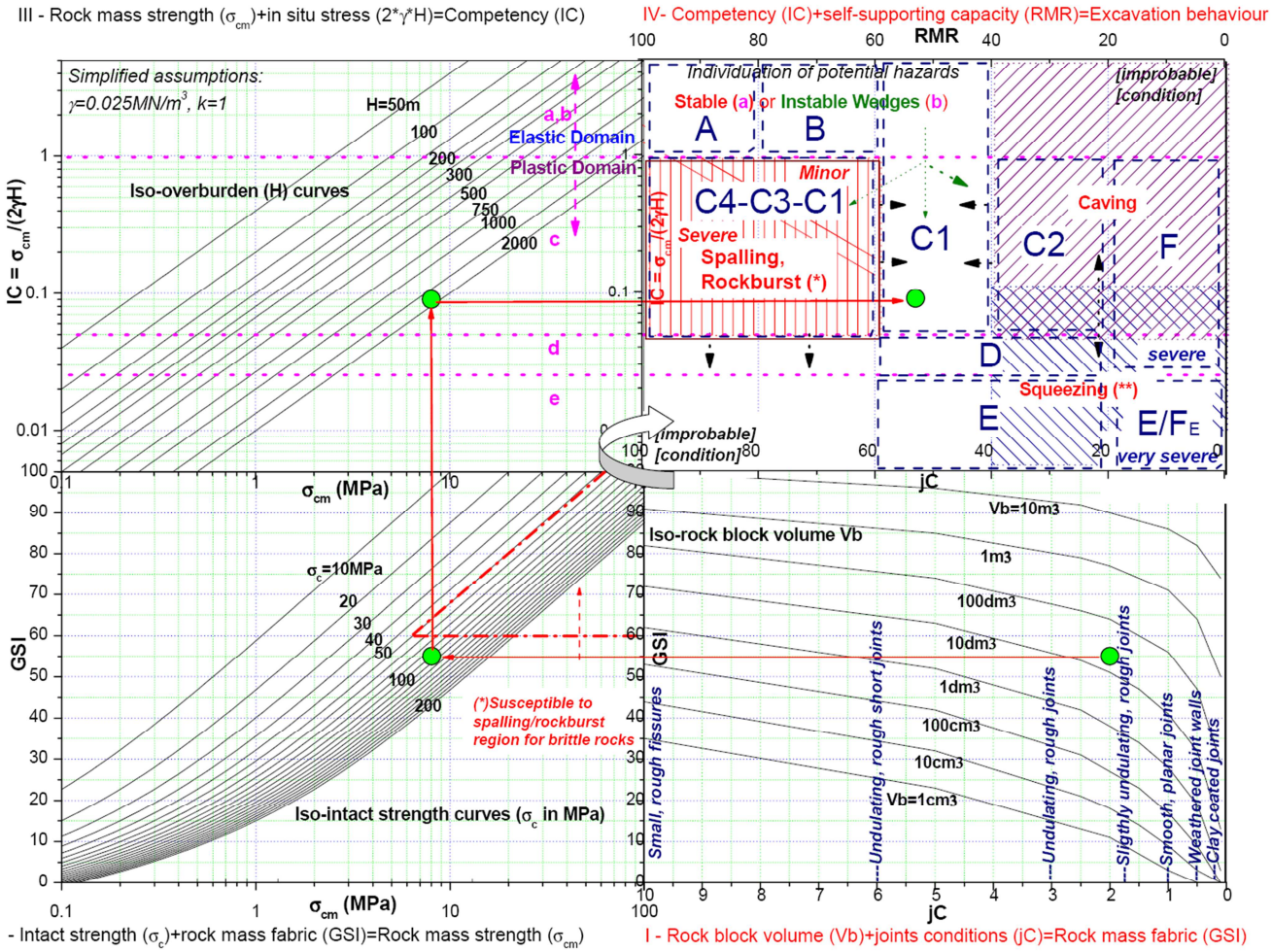

Fig. 9: Example 2 of multiple graph application, showing the GDE usual field of application of the support section types associated to the correspondent regions of hazards. One practical case is remarked on the basis of the estimations done at the tunnel face (proceeding from the I to the IV quadrant):

I_[Vb≈20dm^3 & jC=2 → GSI≈55]; II_[GSI≈55 & σ_c=100MPa → σ_{cm}≈8MPa]; III_[σ_{cm}≈8MPa & $H_{(fictitious)}$ =1750m → IC=0.09]; IV_[IC=0.09 & RMR=53 → (prevalent hazard: wedge instability/rockfall) → Application of the support section type C1].

4 CONCLUSION

An update of the "multiple graph" approach for the preliminary estimate of the rock masses excavation behaviour and, consequently, of the probable hazards for tunnelling has been illustrated.

Such a prediction of the excavation response is obtained by means of the quantification, in a logical sequence, of (1) fabric, (2) strength, (3) competency and (4) self-supporting capacity of rock mass.

Despite the preliminary character of the prediction, which involves some simplified assumptions (for example, circular tunnel in homogeneous/isotropic rock mass, equivalent continuum modelling, k=1,..), the described method may be a useful tool, either in the first phases of design, for a quick identification of potential critical scenarios and for performing sensitivity analysis, and in the construction phase, for the selection of the adequate support section type at the tunnel face on the basis of the pre-defined design criteria.

On the basis of such a preliminary analysis, the tunnel design can consequently focus on the detected potential problems, implementing with the required detail the most adequate methods of analysis and calculations.

5 BIBLIOGRAPHY

[1] Anagnostou, G., Kovari, K., 2003. The stability of tunnels in grouted fault zones, Mitteilungen des Inst. für Geotechnik der ETH, Zürich.
[2] Antolovic, M., Filipovic, A., Amadini, F., 2013. Engineering geological behaviour of rock mass in Chenani Nashri tunnel: the largest road tunnel in India, ITA symposium Croatia, 7-8 May.
[3] Bandis, S.C., 1997. Rock characterization for Tunnelling – A Rock Engineer's Perspective, Feldsbau 15, Nr.3.
[4] Bieniawski, Z.T., 1984. Rock Mechanics Design in Mining and Tunneling, Balkema, Rotterdam, 272pp.
[5] Bieniawski, Z.T., 1989. Engineering Rock Mass Classification, John Wiley & Son.
[6] Cai, M., Kaiser, P.K., H., Tasaka, Y., Minami, M., 2007. Determination of residual strength parameters of jointed rock masses using the GSI system. International Journal of Rock Mechanics & Mining Sciences 44, 247–265.
[7] Carranza-Torres, C., 2004. Elasto-plastic solution of tunnel problems using the generalized form of the Hoek–Brown failure criterion. Proceedings of the ISRM SINOROCK.
[8] Decman, A., Stella, F., Verzani, L.P., 2013. Geomechanical follow-up of El Teniente new mine level access tunnels, ITA symposium Croatia, 7-8 May.
[9] Diederichs, M.S., Kaiser, P.K., Eberhards, E., 2004. Damage initiation and propagation in hard rock during tunnelling and the influence of near-face stress rotation. Int. Journal of Rock Mechanics and Mining Science, Nr.41.
[10] Diederichs, M.S., 2005. General Report: Summary of Meetings with Geodata with recommendations towards a Design Methodology for spalling Failure and Rockburst Hazards, Personal communication.
[11] Diederichs, M.S., Carter, T., Martin, D., 2010. Practical Rock Spall Prediction in Tunnels. ITA World Tunnel Congress Vancouver.
[12] Filipovic, A., Antolovic, M., Angelakis, C., 2013. Design follow-up of Chenani Nashri tunnel construction. ITA symposium Croatia, 7-8 May.
[13] Hoek, E., Brown, E.T., 1980. Underground Excavations in Rock. The Institution of Mining and Metallurgy, London, 527p.
[14] Hoek, E., Diederichs, M., 2006. Estimation of rock mass modulus. Int. Journal of Rock Mechanics and Mining Science.
[15] Hoek, E., Carranza-Torres, C., Diederichs, M.S., Corkum, B., 2008. Integration of geotechnical and structural design in tunnelling. Proc. Univ. of Minnesota 56th Annual Geotechnical Engineering Conference, Minneapolis, 1-53.
[16] Hoek, E., Marinos, P., 2000. Predicting Squeeze. Tunnels and Tunnelling International, November, pp. 45-51.
[17] Hoek, E., Carranza-Torres C., Corkum, B., 2002. Hoek-Brown failure criterion, 2002 Edition. Proc.North American Rock Mechanics Society. Toronto, July 2002.
[18] Hoek, E., Kaiser, P.K., Bawden, W.F., 1995. Support of Underground Excavations in Hard Rock. Balkema, Rotterdam, 215pp.
[19] Kaiser, P.K., 1994. Rockmass failure and implications for support design, 5° Ciclo di Conferenze di Meccanica e Ingegneria delle Rocce a cura di Barla, G., Politecnico di Torino.
[20] Kontrec, P., Constandinidis, V., 2013. Engineering geological characterization of the rock mass in the Adit P4600, Project El Teniente, Chile, ITA symposium Croatia, 7-8 May.
[21] Kovari, K., 1998. Tunnelling in Squeezing Rock, Tunnel Nr.5.
[22] Marinos, P., Hoek, E., 2001. Estimating the geotechnical properties of heterogeneous rock masses such as Flysch Bull. Engg. Geol. Env. 60, 85-92.
[23] Martin, C.D., Kaiser, P.K., McCreath, D.R., 1999, Hoek–Brown parameters for predicting the depth of brittle failure around tunnels. Can. Geotech. Journal 36, 136–151.
[24] Palmstrom, A., 1996. Characterizing rock masses by the RMi for use in practical rock engineering. Tunn. and Und. Space Tech., vol.11.
[25] Palmstrom, A., 2000. Recent developments in rock support estimates by the RMi. Journal of Rock mechanics and tunneling technology, Vol. 6, 1-9.
[26] Palomba, M., Russo, G., Amadini, F., Carrieri, G., Jain, A.R., 2013. Chenani-Nashri Tunnel, the longest road tunnel in India: a challenging case for design-optimization during construction . World Tunnel Congress, Geneva.
[27] Russo, G., Kalamaras, G.S., Grasso P., 1998. A discussion on the concepts of geomechanical classes, behavior categories and technical classes for an underground project. Gallerie e grandi opere sotterranee, Nr. 54, 40-51.
[28] Russo, G., Grasso, P., 2006. Un aggiornamento sul tema della classificazione geomeccanica e della previsione del comportamento allo scavo. Gallerie e grandi opere sotterranee, Nr. 80, 56-65.
[29] Russo, G., Grasso, P., 2007. On the classification of the rock mass excavation behaviour in tunnelling Proc. 11th Congress of ISRM, Lisbon, pp 979-982.
[30] Russo, G., 2007. Improving the reliability of GSI estimation: the integrated GSI-RMi system. Proc. I.S.R.M. Workshop "Underground Works under Special Conditions", Madrid, pp 123-130.
[31] Russo, G., 2008. A simplified rational approach for the preliminary assessment of the excavation behaviour in rock tunnelling. Tunnels et Ouvrages Souterraines, n. 207, mai-juin.
[32] Russo, G., 2009. A new rational method for calculating the GSI. Tunnelling and Underground Space Technology n.24, pp.103-111.
[33] Tzamos, S., Sofianos, A.I., 2007. A correlation of four rock mass classification systems through their fabric indices. Intern. Journal of Rock Mechanics and Mining.

[Note in the following the full-page Multiple Graph]

III - Rock mass strength (σ_{cm})+in situ stress ($2*\gamma*H$)=Competency (IC)

IV- Competency (IC)+self-supporting capacity (RMR)=Excavation behaviour

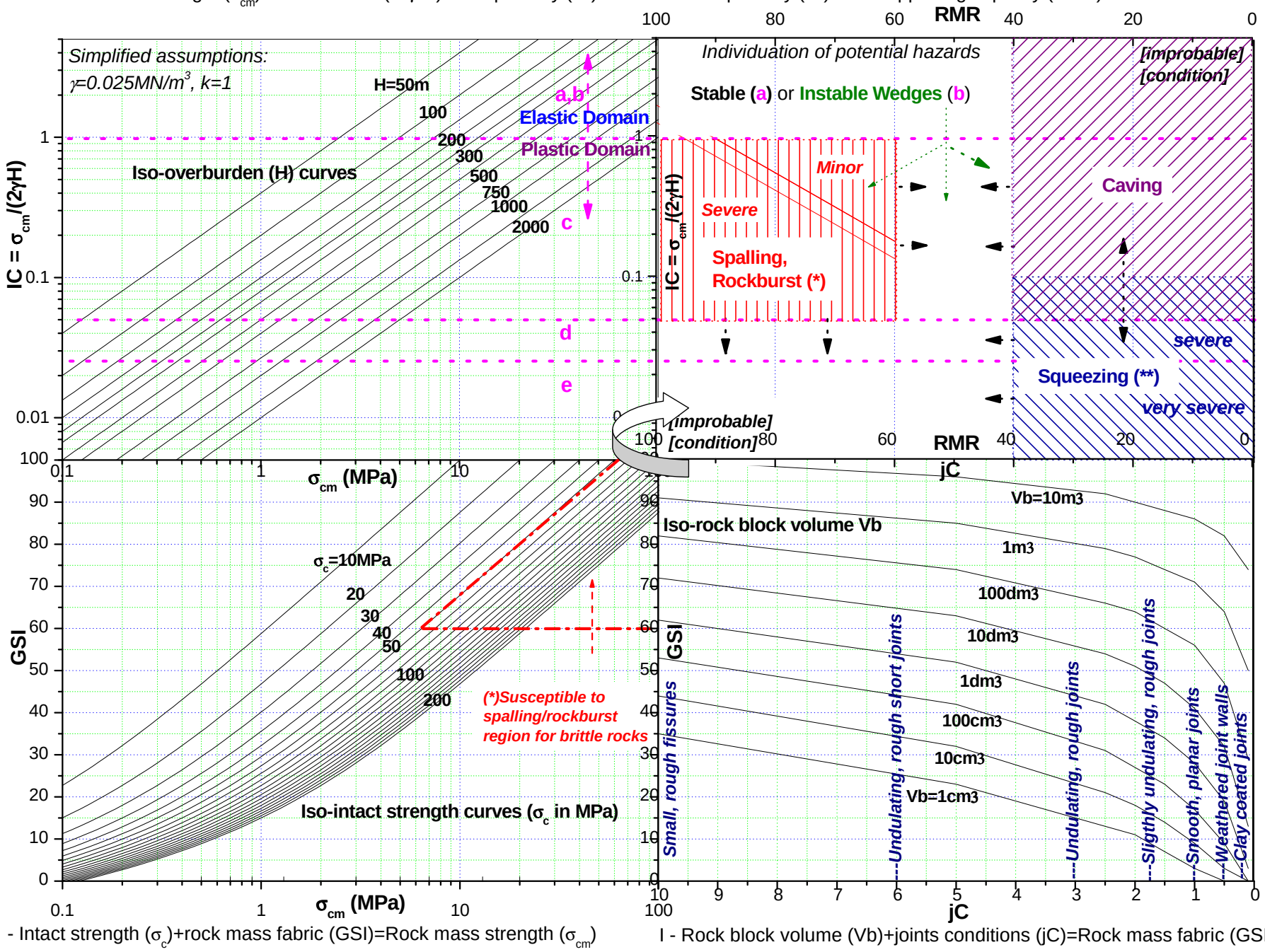

II - Intact strength (σ_c)+rock mass fabric (GSI)=Rock mass strength (σ_{cm})

I - Rock block volume (Vb)+joints conditions (jC)=Rock mass fabric (GSI)

(*) only for the susceptible region, otherwise the development of plastic region and moderate radial convergences are more probable

(**) depending also from the length of the potential proned zone: given a possible "silo effect", for short zones included in good quality rocks, a caving behaviour it is most likely